APPLICATION OF THE DIAGRAM TECHNIQUE TO THE HEISENBERG FERROMAGNET WITH CRYSTAL FIELD ANISOTROPY. SPIN 1

BY M. MATLAK AND B. WESTWAŃSKI

Institute of Physics, Silesian University, Katowice*

(*Received July 24, 1972; Revised paper received November 22, 1972*)

Spin diagram technique of Izyumov and Kassan-Ogly is applied to the Heisenberg ferromagnet with anisotropy of the type $-K\sum_f(S_f^z)^2$. Complementary rules for diagrams are given. When using this technique the well known results of Lines, Noskova, Devlin, Potapkov and correspondence between decoupling scheme for the Green functions and some classes of diagrams are obtained.

1. Introduction

In papers [1a, b] Izyumov and Kassan-Ogly have formulated very convenient spin diagram technique for the Heisenberg ferromagnet. This diagram technique was based on the analogy of the Wick's theorem for the spin operators [2], [1a, b]. The spin diagram technique has been used for considerations of antiferromagnet in [1a], ferromagnet in [1b] and *s–d* model in [1c].

In our paper we have to do with the spin system described by the Hamiltonian

$$H = -h\sum_f S_f^z - \tfrac{1}{2}\sum_{f\neq g} J_{fg}(S_f^- S_g^+ + S_f^z S_g^z) - K\sum_f (S_f^z)^2, \tag{1}$$

where the first term is Zeeman's energy, the second-exchanceg interaction and the third is single ion anisotropy. Everything we know about thermodynamical properties of such systems may be found in papers [3]–[7]. These authors worked in the frame work of the theory of the equations of motion for the double-time Green functions. All the authors [4]–[7] have taken into consideration the single ion anisotropy term exactly applying only the usual Tyablikov decoupling procedure to the Green functions containing the spin operators with different lattice sites. Lines [3] has applied a special kind of the decoupling scheme to the Green functions constructed with the spin operators from single ion aniso-

* Address: Instytut Fizyki, Uniwersytet Śląski, Uniwersytecka 4, 40-007 Katowice, Poland.

tropy. For the other Green functions he has used Tyablikov decoupling procedure. His decoupling method does not take into account the crystal field anisotropy strictly. Let us discuss this. The use of the spin diagram technique allows us to obtain all results of Refs [3]–[6]. It shows equivalence between the decoupling procedure used in [3]–[6] and the summation of certan classes of graphs.

In § 2 we recall very briefly the essence of the spin diagram technique of Izyumov and Kassan–Ogly.

In § 3 we supplement the diagram technique due to our case.

In § 4 we perform the summation of certain classes of graphs to obtain the results of [4]–[6].

In § 5 we sum the graphs to have the result of [3].

2. *Spin diagram technique*

The starting point of the spin diagram technique is the formulation of the Wick's theorem for the spin operators [2], [1a, b]. According to this theorem every statistical average of n "time" ordered spin operators can be expressed by the sum of the statistical averages of $n-1$ "time" ordered products each of them multiplied by the Green function of the type

$$G_0(\tau-\tau') = \frac{\langle TS^-(\tau)S^+(\tau')\rangle_0}{2\sigma_0} = e^{h(\tau-\tau')}\begin{cases} n_\beta & \tau > \tau' \\ n_\beta+1 & \tau < \tau' \end{cases} \tag{2}$$

where $\sigma_0 = \langle S^z\rangle_0$ is the magnetization and $n_\beta = (e^{\beta h}-1)^{-1}$. This procedure may be repeated for every term with $n-1$ operators and so on. In the end every statistical average of n "time" ordered spin operators becomes a sum of terms each at them being a product of some number of the Green functions (2) and a statistical average of a number of the operators S^z. Each such term can be represented graphically. Any graph is made up of the following parts: wavy lines, directed lines, single points and ovals. Exchange integral J_{fg} we denote as a wavy line, Green function (2) as directed line $\tau \longrightarrow \tau'$. Directed lines and isolated points form bloks. When bloks have the same lattice site index we put them in oval. Each oval gives the contribution $\sigma_0^{(\alpha-1)} \equiv \dfrac{d^{\alpha-1}\sigma_0}{d(\beta h)^{\alpha-1}}$, where α is a number of different parts in an oval. The whole contribution from an n-order graph can be expressed in the form [1a, b]

$$(-1)^F 2^m \frac{P_n}{2^n n!} \prod_s \sigma_0^{[\alpha_s-1]} \int_0^\beta d\tau_1 \int_0^\beta d\tau_2 \ldots \int_0^\beta d\tau_n \sum_{f_1\neq g_1} \sum_{f_2\neq g_2} \ldots \sum_{f_n\neq g_n} J_{f_1g_1} J_{f_2g_2} \ldots$$

$$\ldots J_{f_ng_n} G_0(\ldots) \ldots G_0(\ldots)\delta(\ldots) \ldots \delta(\ldots). \tag{3}$$

F is the number of points at which one or two directed lines come together and one directed line goes out, m is the number of points from which the directed line go out, P_n is the number of topologically equivalent graphs, α_s—the number of different parts in an S-oval. This can be seen in more detail in [1a, b].

This diagram technique is much simpler and more convenient than that of Stinchcombe *et al.* [8].

3. *Spin diagram technique for Heisenberg ferromagnet with crystal field anisotropy*

In contrast to § 1 owing to the existence of the additional term $-K\sum_f (S_f^z)^2$ in (1), the diagram technique [1a, b] should be supplemented. To do it consider for example the average

$$\langle TS_m^-(\tau)S_n^+(\tau')\rangle = \sum_{l=0}^{\infty} \frac{(-1)^l}{l!} \int_0^\beta d\tau_1 \dots \int_0^\beta d\tau_l \langle TV(\tau_1) \dots V(\tau_l) S_m^-(\tau) S_n^+(\tau')\rangle_{oc}, \tag{4}$$

where

$$V(\tau_i) = e^{\tau_i H_0} V e^{-\tau_i H_0}, \tag{5}$$

$$H_0 = -h \sum_f S_f^z, \tag{6}$$

and

$$V = -\tfrac{1}{2} \sum_{f \neq g} J_{fg}(S_f^- S_g^+ + S_f^z S_g^z) - K \sum_f (S_f^z)^2. \tag{7}$$

$\langle \dots \rangle_o = \dfrac{\mathrm{Tr}\,(e^{-\beta H_0} \dots)}{\mathrm{Tr}\, e^{-\beta H_0}}$ and $\langle \dots \rangle_{oc}$ denotes the connected average. To represent the right-hand side of (4) graphically we design $K\sum_f (S_f^z)^2$ as O----O. Linked cluster expansion contains the graphs related to exchange interaction, single ion anisotropy and both. The graphs of the first type are well known [1a, b] and theorefore are not considered here. Because the third kind graphs may be constructed be means of previous types we restrict ourselves to the investigation of the second kind only. It should be noticed that if there is to be no exchange interaction we have graphs of the second kind solely. In the first order of Eq. (4) we have the term

$$K \sum_{f_1} \int_0^\beta d\tau_1 \langle T(S_{f_1}^z(\tau_1))^2 S_m^-(\tau) S_n^+(\tau')\rangle_{oc}. \tag{8}$$

Drawing all possible contractions of all operators (graphical representation of the Wick's theorem [2], [1a, b]) in (8), we get

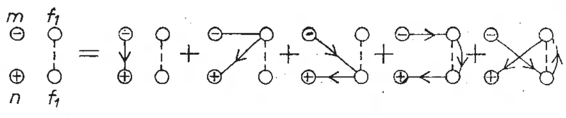

(9)

It is easy to see that

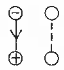

$$= 2\beta K\delta_{mn} \sum_{f_1} \langle S^z_m (S^z_{f_1})^2\rangle_{oc}\, G_0(\tau-\tau'), \qquad (10)$$

where

$$\langle S^z_m (S^z_{f_1})^2\rangle_{oc} = \delta_{mf_1}(\sigma_0''+2\sigma_0'\sigma_0), \qquad (11)$$

and $\sigma_0 \equiv \sigma_{0m}$ for every lattice site index m.

Taking into account (10) and (11) we can express (10) in terms of connected diagrams as follows

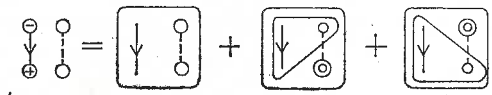

(12)

where

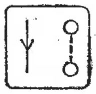

$$= 2\beta K\delta_{mn}\,\sigma_0''\quad G_0(\tau-\tau'), \qquad (13)$$

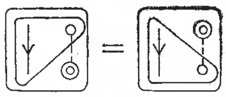

$$= 2\beta K\delta_{mn}\,\sigma_0'\sigma_0\, G_0(\tau-\tau'), \qquad (14)$$

From (13) we see that $K(S^z_f)^2 =$ O----O should be treated as 2 different blocks. Therefore the oval (13) contains now three blocks and according to [1a, b] we have σ_0''. In all further considerations we will assume that O----O means two different blocks. We used in (14) double ovals. The external oval shows that all operators in it have the some lattice site index. Proceeding analogically as in (10) and (11) with the other contractions in (9) we have

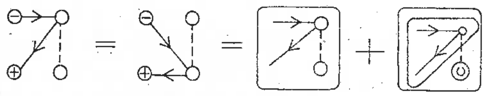

(15)

where

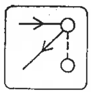

$$= -2K\sum_{f_1}\delta_{mf_1}\delta_{f_1 n}\,\sigma_0' \int_0^\beta d\tau_1\, G_0(\tau-\tau_1)\, G_0(\tau_1-\tau') \qquad (16)$$

and

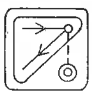

$$= -2K\sum_{f_1}\delta_{mf_1}\delta_{f_1 n}\,\sigma_0^2 \int_0^\beta d\tau_1\, G_0(\tau-\tau_1)\, G_0(\tau_1-\tau') \qquad (17)$$

For the last two terms of (9) we get

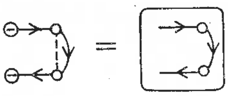

$$= 2K\sum_{f_1}\delta_{mf_1}\delta_{f_1 n}\,\sigma_0 G_0(+0) \int_0^\beta d\tau_1\, G_0(\tau-\tau_1)\, G_0(\tau_1-\tau') \qquad (18)$$

and

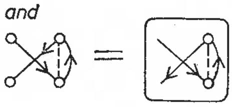

$$= 2K\sum_{f_1}\delta_{mf_1}\delta_{f_1 n}\,\sigma_0 G_0(-0) \int_0^\beta d\tau_1\, G_0(\tau-\tau_1)\, G_0(\tau_1-\tau') \qquad (19)$$

We make an arrangement in all further cases that if the directed line is going down or up then it gives the contribution $G_0(+0)$ or $G_0(-0)$ respectively.

In the second and higher orders of (4) there are more and more graphs. All these graphs can be obtained in very much the same way as (9). In addition to the rules of [1a, b] we have to introduce the following rules. Namely O---O should be treated as two blocks and the operators $S_f^z(\tau)$ in O----O may be connected in two ways by the directed line. When a directed line is going up then contributes to $G_0(-0)$ and when the line is going down it gives $G_0(+0)$. Moreover several ovals should be surrounded by the external oval when the lattice index is the same.

4. *Results of Refs* [4]–[6]

We take into considerations two functions:

$$A_{m-n}(\tau-\tau') \equiv \langle TS_m^-(\tau)\, S_n^+(\tau')\rangle \text{ and } B_{m-n}(\tau-\tau') \equiv \langle TS_m^2(\tau)\, S_m^-(\tau) S_n^+(\tau')\rangle .$$

First we compute the function $A_{mn}(\tau-\tau')$. For this purpose we define the Fourier space and "time" transformation

$$A_{n-n}(\tau-\tau') = \frac{1}{N}\cdot\frac{1}{\beta}\sum_k \sum_{\omega_p} e^{ik(m-n)} e^{-i\omega_p(\tau-\tau')} A_k(\omega_p), \tag{20}$$

where

$$A_k(\omega_p) = \tfrac{1}{2}\sum_m e^{-ikm} \int_{-\beta}^{\beta} d\tau e^{i\omega_p \tau} A_m(\tau). \tag{21}$$

The same can be made with the function $B_{m-n}(\tau-\tau')$. The perturbation series for $A_k(\omega_p)$ in terms of diagrams is given in Appendix Ia. First we sum the diagrams from Appendix Ia giving the contribution in n-th order proportional to $\dfrac{J_0^n}{(i\omega_p+h)^{n+1}}$, where $J_0 = \sum_g J_{fg}$. The sum of these graphs (Appendix Ib) is

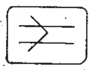

$$\equiv \frac{2\sigma_0}{i\omega_p+h}\sum_{n=0}^{\infty}(-1)^n\left(\frac{\sigma J_0}{i\omega_p+h}\right)^n = \frac{2\sigma_0}{i\omega_p+h+\sigma_0 J_0}. \tag{22}$$

Consider now the graphs from Appendix Ia giving the contribution in n-th order proportional to $\dfrac{k^n}{(i\omega_p+h)^{n+1}}$ (Appendix Ic).

We obtain

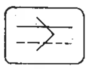

$$\equiv \frac{2\sigma_0}{i\omega_p+h} + \frac{\lambda_0}{i\omega_p+h}\sum_{n=1}^{\infty}\left(\frac{K}{i\omega_p+h}\right)^n ((-1)^n-1)+$$

$$+\frac{\sigma_0}{i\omega_p+h}\sum_{n=1}^{\infty}\left(\frac{K}{i\omega_p+h}\right)^n (1+(-1)^n) = \frac{2\sigma_0(i\omega_p+h)-2\lambda_0 K}{(i\omega_p+h)^2-K^2}. \tag{23}$$

Let us now collect from Appendix Ia the graphs with the contribution in n-th order proportional to $\frac{(J^k)^n}{(i\omega_p+h)^{n+1}}$ (Appendix Id).

We get

$$\equiv \frac{2\sigma_0}{i\omega_p+h}\sum_{n=0}^{\infty}\left(\frac{\sigma_0 J_k}{i\omega_p+h}\right)^n = \frac{2\sigma_0}{i\omega_p+h-\sigma J_k},$$

where

$$J_k = \sum_m J_m e^{-ikm}, \quad J_{fg} = J_{f-g}. \tag{24}$$

We renormalize the series (23) with help of (22) replacing each directed line $\longrightarrow$ in (23) by $\Longrightarrow$ from (22).

We obtain

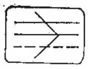

$$\equiv \frac{2\sigma_0(i\omega_p+h+\sigma_0 J_0)-2\lambda_0 K}{(i\omega_p+h+\sigma_0 J_0)-K^2}. \tag{25}$$

We replace now each directed line $\longrightarrow$ in (24) by $\Longrightarrow$ from (25). If one renormalizes additionally the ovals in (22), (23) and (24) one obtains instead of σ_0 and λ_0 full σ and λ. Therefore we can write

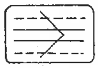

$$\equiv A_k(\omega_p) =$$

$$= \frac{2\sigma(i\omega_p+h+\sigma J_0)-2\lambda K}{(i\omega_p+h)^2+\sigma(2J_0-J_k)(i\omega_p+h)+\sigma^2 J_0^2-\sigma^2 J_0 J_k+\lambda K J_k-K^2}. \tag{26}$$

Now we shall be interested in the function $B_{m-n}(\tau-\tau')$. For the Fourier transform of this function we have the linked cluster expansion in Appendix IIa. The partial summation of diagrams from Appendix IIa needed for getting suitable results may be obtained in the following way. We first sum the diagrams with contribution proportional to $\frac{J_0^n}{(i\omega_p+h)^{n+1}}$ in n-th order (Appendix IIb). This sum is

$$(IIb) = \frac{\lambda_0-\sigma_0}{i\omega_p+h+\sigma_0 J_0}. \tag{27}$$

Next we sum the diagrams contributing in n-th order proportional to $\frac{K^n}{(i\omega_p+h)^{n+1}}$ (Appendix IIc). We get

$$(IIc) = \frac{\lambda_0-\sigma_0}{i\omega_p+h-K}. \tag{28}$$

After renormalizing the graphs in (27) by means of (28) we obtain the result

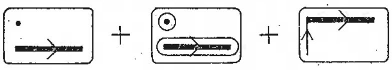

$$\equiv \frac{\lambda_0-\sigma_0}{i\omega_p+h+\sigma_0 J_0-K} \cdot \quad (29)$$

Consider now the following series

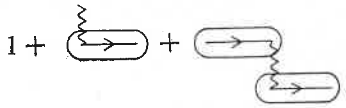

$$= \frac{1}{1-\sigma_0 J_k G_k^0} \cdot \quad (30)$$

We can renormalize the series (30) replacing the directed line  by 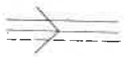 form (25).

Finally we sum the series

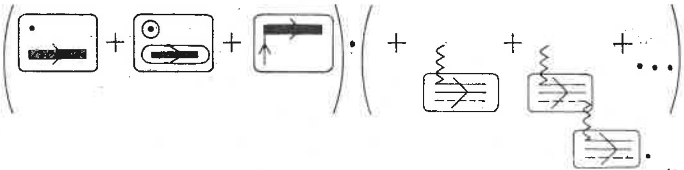

(31)

After renormalizing the ovals in (31) we obtain full σ and λ instead of σ_0 and λ_0. Therefore the expression for $B_k(\omega_p)$ obtained from (31) is

$$B_k(\omega_p) = \frac{(\lambda-\sigma)(i\omega_p+h+\sigma J_0+K)}{(i\omega_p+h)^2+\sigma(2J_0-J_k)(i\omega_p+h)+\sigma^2 J_0^2-\sigma^2 J_0 J_k+\lambda K J_k-K^2} \cdot \quad (32)$$

By means of (26) and (32) we obtain two equations for σ and λ. These equations are the same as those obtained in Refs [4]–[6] and therefore we can say that the way of summation to get (26) and (32) is simply equivalent to the decoupling scheme used in [4]–[6].

5. *Decoupling procedure of Lines*

Lines [3], applying a special decoupling procedure has found

$$A_k(\omega_p) = \frac{2\sigma}{i\omega_p+h+\sigma(J_0-J_k)+\dfrac{\lambda}{\sigma}K} \quad (33)$$

where $\lambda = 3\langle (S^z)^2\rangle - S(S+1)$.

To obtain the result (33) for $S=1$ with the aid of the diagram technique we have to assume $K \ll 1$. In this case we omit in (23) the terms proportional to K^n, $n>1$. From (23) we have

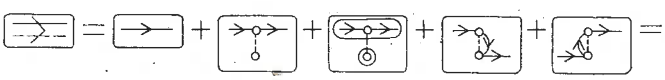

$$= \frac{2\sigma_0}{i\omega_p+h} - \frac{2\lambda_0 K}{(i\omega_p+h)^2} \approx \frac{2\sigma_0}{i\omega_p+h+\dfrac{\lambda_0}{\sigma_0}K} \cdot \quad (34)$$

We renormalize each directed line in (34) by means of (22) and we obtain

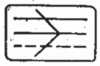

$$\approx \frac{2\sigma_0}{i\omega_p + h + \sigma_0 J_0 + \frac{\lambda_0}{\sigma_0} K} \qquad (35)$$

Replacing now each directed line  in (24) by  from (35) we get (33) but with $\sigma = \sigma_0$ and $\lambda = \lambda_0$. To have (33) we must additionally renormalize all the ovals in (22), (34) and (24).

We see that the approximation of Lines is valid when the coupling constant K is small.

APPENDIX I[1]

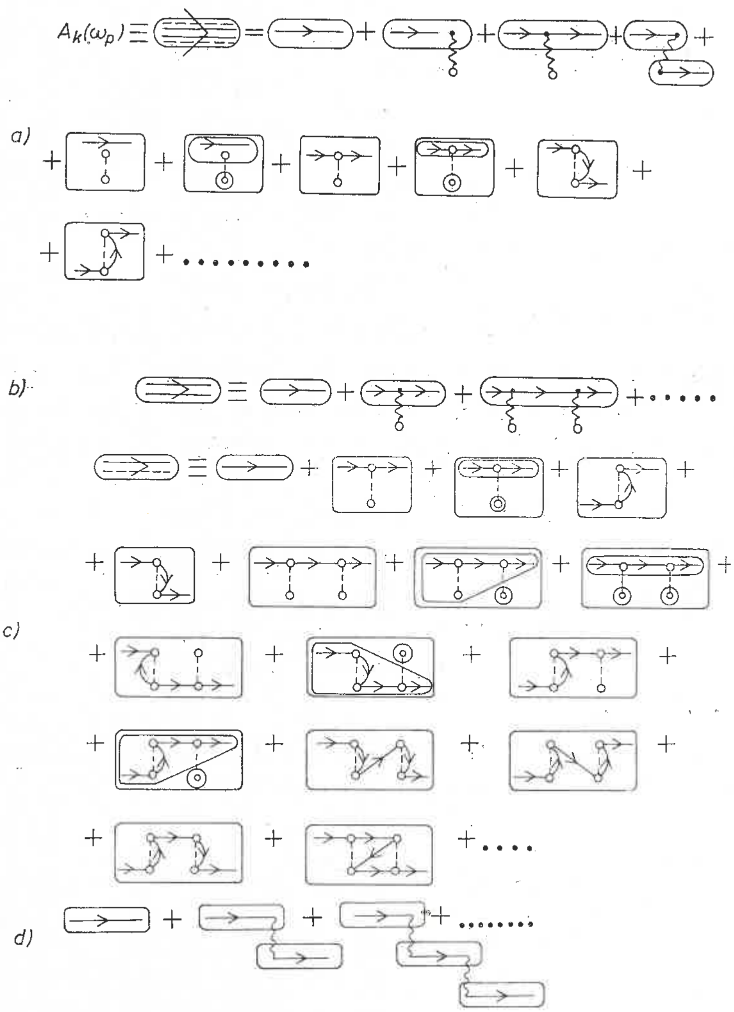

[1] We draw topologically inequivalent graphs

APPENDIX II

a) $B_k(\omega_p) \equiv$

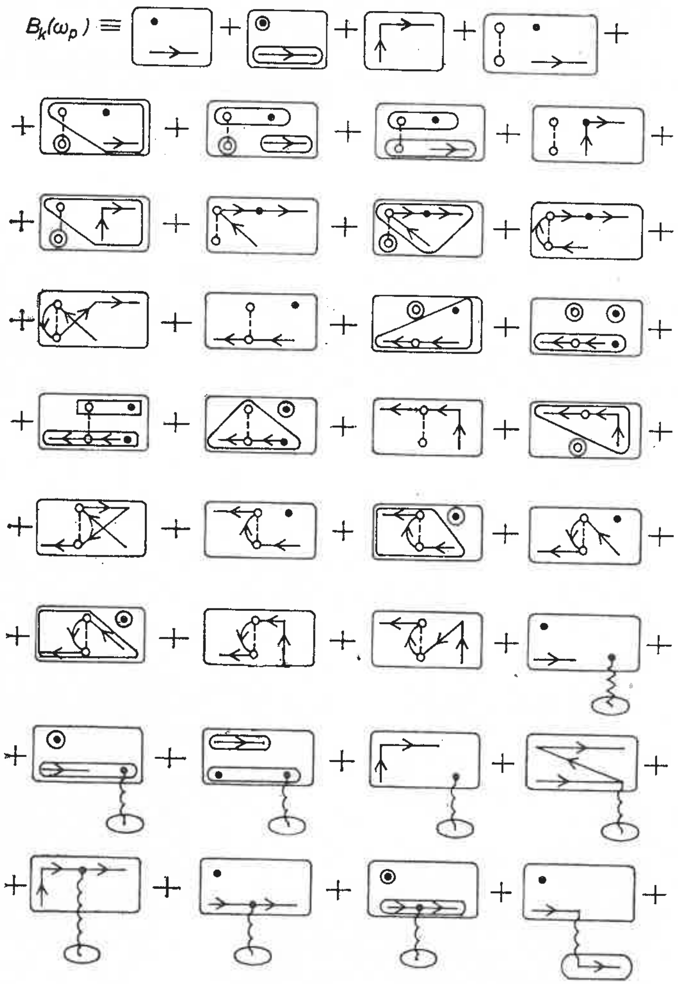

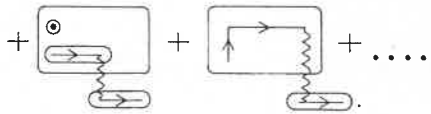

b)

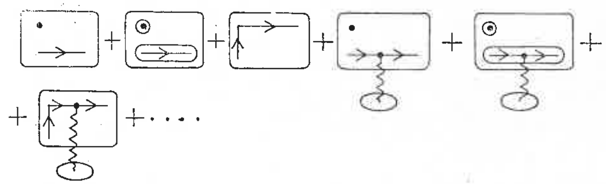

c)

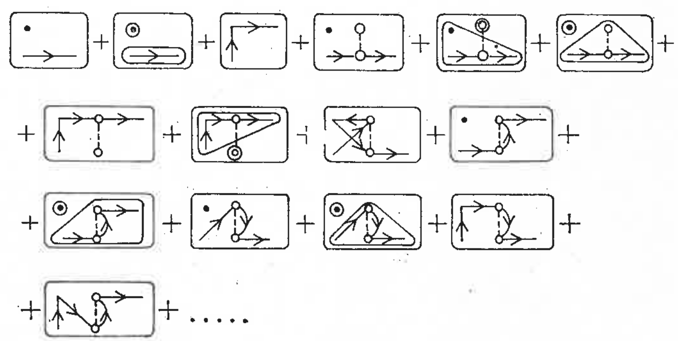

6. *Conclusions*

We have obtained the results of Refs [3]–[6] using the spin diagram technique. This technique, however, is not particularly convenient because of the great number of graphs coming from the crystal field anisotropy. It is not so easy, in some cases, to calculate the invers Fourier "time" transform of the contributions from these kind graphs. It is possible to reduce the number of graphs and to improve this technique. This will be given in the next paper.

We wish to thank Dr A. Pawlikowski for helpful discussions.

REFERENCES

[1] Yo. A. Izyumov, P. A. Kassan-Ogly, a) *Fiz. Metallov Metallovedenie*, **26**, 385 (1968); b) *Fiz. Metallov Metallovedenie*, **30**, 225 (1970); c) *Preprint*, Dubna 1969.
[2] V. G. Vaks, A. J. Larkin, S. A. Pikin, *Zh. Eksper. Teor. Fiz.*, **53**, 281, 1089 (1967).
[3] M. E. Lines, *Phys. Rev.*, **156**, 534 (1969).
[4] L. M. Noskova, *Fiz. Metallov Metallovedenie*, **33**, 698 (1972).
[5] J. F. Devlin, *Phys. Rev.*, **B4**, 136 (1971).
[6] N. A. Potapkov, *Theor. Math. Phys.* (USSR), **8**, 381 (1971).
[7] M. Matlak, K. Skrobiś, *Acta Phys. Polon.*, **A42**, 413 (1972).
[8] R. L. Stinchcombe, G. Horwitz, F. Englert, R. Brout, *Phys. Rev.*, **130**, 155 (1963).